https://doi.org/10.5194/essd-2026-141
Preprint. Discussion started: 19 March 2026

Open Access Earth System Science Data Discussions

Coordinated methane flux measurements from northern lakes by the SITES Water program - open data and learning examples

David Bastviken[1], Blaize A. Denfeld[2], Holger Villwock[2], Jonathan Schenk[3], Leif Klemedtsson[4], Hjalmar Laudon[5], Niels Aagard Jakobsen[6], Stefan Bertilsson[2], Kevin Bishop[2], William Colom Montero[7], Silke Langenheder[7], Amelie Lindgren[4], Erik Lundin[8], Niklas Rakos[8], Johannes Tiwari[9], Per Weslien[4], Marcus B. Wallin[2]

[1]Department of Thematic Studies - Environmental Change, Linköping University, Sweden
[2]Department of Aquatic Sciences and Assessment, Swedish University of Agricultural Sciences, Uppsala, Sweden
[3]Department of Physical Geography and Ecosystem Science, Lund University, Lund Sweden
[4]Department of Earth Sciences, University of Gothenburg, Gothenburg, Sweden
[5]Department of Forest Ecology and Management, Swedish University of Agricultural Sciences, Umeå, Sweden
[6]Unit for Field-based Forest Research, Asa Research Station, Swedish University of Agricultural Sciences, Lammhult, Sweden
[7]Department of Ecology and Genetics, Limnology, Uppsala University, Uppsala, Sweden
[8]Abisko Scientific Research Station, Swedish Polar Research Secretariat, Abisko, Sweden
[9]Unit for Field-based Forest Research, Vindelns Research Park, Swedish University of Agricultural Sciences, Vindeln, Sweden

Correspondence to: David Bastviken (david.bastviken@liu.se), Marcus Wallin (marcus.wallin@slu.se)

Abstract. Lakes represent one of the main sources of methane (CH_4) to the atmosphere, contributing roughly 3-25% of the total global yearly emissions. While the scientific interest in understanding and modelling these emissions is increasing rapidly, methodologically consistent long-term flux measurement programs of integrated lake CH_4 emissions are largely missing. Here we present results from a systematic and comparable spatiotemporal multi-lake CH_4 flux program initiated by the Swedish Infrastructure for Ecosystem Science (SITES). Five lakes distributed across Sweden covering a latitudinal gradient from 68°N to 57°N, including the arctic subalpine, boreal and north temperate zones, were monitored during 2016-2022 in ways that captured variability in space and time within lakes and that allowed between-lake comparisons. The data includes 2375 unique CH_4 flux measurements (incl. total CH_4 fluxes, diffusive fluxes and surface water concentrations) along with other common physical and chemical lake variables. This paper presents these data (Swedish Infrastructure for Ecosystem Science, 2026, https://doi.org/10.23700/05ax-st65), underlying methodological priorities and procedures, and provides examples of what can be learned from such a coordinated sampling program. Briefly, the data show the need for appropriate consideration of ebullition and space-time integration to properly represent whole lake CH_4 fluxes. The data further show that both diffusive and total CH_4 fluxes have an apparent temperature dependency, which can be modulated by water depth in ways that differ among lakes. Also, yearly open water CH_4 flux estimates were consistently shaped by temperature in all lakes, but the strength of this response differed between lakes; increases of whole season mean water temperature between 0.5 and 3.2°C corresponded to increases in CH_4 fluxes ranging from 16 to 74%. Finally, we propose that temperature-normalized CH_4 fluxes should be used in lake emission inter-comparisons.

https://doi.org/10.5194/essd-2026-141
Preprint. Discussion started: 19 March 2026

Open Access Earth System Science Data Discussions

1 Introduction

Freshwater lakes represent one of the largest sources of the greenhouse gas (GHG) methane (CH_4) to the atmosphere. The reported global emission estimates range from 22-151 Tg yr^{-1}, corresponding to 3-25% of the global CH_4 emissions (mean range of 575-669 Tg yr^{-1} (Johnson et al. 2022; Saunois et al. 2025). The broad range in estimated flux reflects a large uncertainty that undermines our understanding of the global CH_4 budget (Kirschke et al. 2013; Saunois et al. 2025). This uncertainty can be linked to (1) lake surface estimates, (2) extrapolation approaches, and (3) the mix of flux measurement designs underlying the data combined for global emission estimates (Johnson et al. 2022; Saunois et al. 2025).

The main flux types for CH_4 across the water surface are bubble flux from the sediments (ebullition) and flux of dissolved CH_4 in water across the diffusive surface boundary layer to the atmosphere (diffusive flux). Ebullition typically dominates small lakes with certain sediments, while diffusive flux can be significant in larger lakes or where sediment characteristics do not favor bubble formation or release (Bastviken et al. 2004). The difference between these flux types has important implications for measurement designs. Ebullition based on sediment CH_4 production (as opposed to bubbling of CH_4 from deep geogenic sources) can be a highly irregular and semi-stochastic process in time and space. Production rates of CH_4 in sediments determine bubble buildup until sudden bubble release after reaching a critical buoyancy in relation to sediment characteristics. Bubbling events can be triggered locally by such bubble growth or at larger scales by disturbances such as pressure changes (Mattson and Likens 1990). After ebullition events, it typically takes time to build up sediment CH_4 bubbles again, resulting in legacy effects. Hence, the episodic ebullition emissions, which can happen in seconds, correspond to several days of production with the timing and location being difficult to predict. Ebullition fluxes thereby represent large but rare outliers in floating flux chamber datasets that can account for 50 to >90% of the total flux locally (Bastviken et al. 2004, Sø et al. 2025). Accordingly, accurate measurements of ebullition need to cover enough space and time to representatively capture these rare outlier events (Wik et al. 2016).

Diffusive flux, on the other hand, is regulated by the balance of (1) CH_4 inputs, including formation rates, re-dissolution of passing bubbles, and other inputs via, e.g. groundwater, and (2) CH_4 losses, including CH_4 oxidation and recent losses by emission, e.g. if a recent storm depleted dissolved surface water CH_4 by increasing turbulence and thereby the gas transfer velocity across the diffusive boundary (MacIntyre et al. 2019; 2021). Various in-lake transport patterns at scales ranging from seasons to minutes shape this balance by transporting CH_4 and regulating residence times under which CH_4 oxidation can influence concentrations (DelSontro et al. 2018). Diffusive flux is dynamic but continuous, compared to ebullition, and can be representatively measured with less coverage of time and space (Wik et al. 2016).

The complex regulation of ebullition and diffusive flux makes it challenging to reach conclusive information about how CH_4 emissions may change over time. Furthermore, there is growing support for a positive effect of aquatic primary productivity

https://doi.org/10.5194/essd-2026-141
Preprint. Discussion started: 19 March 2026

and nutrient levels on CH_4 emissions (Davidson et al. 2018; DelSontro et al. 2016). The likely reason is that greater inputs of freshly produced and readily accessible organic substrates for use by methanogenic archaea and their bacterial support systems can enhance whole-system CH_4 production (Grasset et al. 2018). This points towards predictable patterns in CH_4 emissions among lakes and with changing nutrient levels, while quantification *in situ* remains a challenge given the widely different measurement designs for different lakes and the general scarcity of long-term measurements.

Several *in situ* studies have shown an exponential increase in ebullition with increasing temperature (Wik et al. 2016; Aben et al. 2017; Natchimuthu et al. 2016). This aligns with the strong temperature dependence for methanogenesis (Yvon-Durocher et al. 2014; Marotta et al. 2014), which is key for bubble formation rates in sediments. For diffusive CH_4 flux, the situation has so far been unclear. Mechanistically, diffusive flux is influenced by many different biochemical and physical processes that are regulated in different ways, making theoretical links to temperature responses obscure and elusive. In terms of total net *in situ* diffusive flux, some studies with extensive space-time coverage of measurements on individual lakes, suggest that diffusive flux may also respond positively to temperature (Natchimuthu et al. 2016, Rasilo et al. 2014). However, other studies do not report a clear temperature response for diffusive flux (Aben et al. 2017).

On top of the spatiotemporal complexity, there may be space-time interactions. One example is that the seasonal temperature impacts on ebullition and total emissions may be greater in near-shore shallow parts of lakes where sediments are exposed to the surface mixed layer and where water temperatures reflect air temperatures. Seasonal temperature responses may instead be smaller and largely related to diffusive flux at deeper lake parts (Natchimuthu et al. 2016). Such interactions could generate widely different results between studies with measurements of mainly deep waters versus measurements that are distributed across the entire range of depths in a lake.

To improve our understanding of dynamics and regulation of lake CH_4 emissions over time, measurement designs need to account for temporal variability within and among seasons and over several years, as well as spatial variability within individual lakes. In addition, consistent methodology needs to be applied in multiple lakes to enable comparisons between ecosystems. Such efforts are difficult to maintain with normal 3-5-year research projects and typically require longer and larger research programs which are rare. Here we present data from the Swedish Infrastructure for Ecosystem Science (SITES) that encompass systematic and comparable spatiotemporal CH_4 flux measurements of to seven years for five lakes distributed from the arctic to north temperate region.

2 The SITES Water GHG Flux Program

SITES is a distributed national research infrastructure consisting of field stations that enable ecosystem research that cuts across climate zones, landscape elements and land use management within Sweden. One component of the infrastructure is

https://doi.org/10.5194/essd-2026-141
Preprint. Discussion started: 19 March 2026

the Thematic Program SITES Water, a coordinated catchment monitoring program of lakes and streams associated with the SITES research stations. Within SITES Water, a Greenhouse Gas Flux Program (henceforth referred to as SITES Water GHG Flux Program) was implemented at five lakes and has been running since 2016. Here we present data collected during the period 2016-2022 and exemplify how the data can be used to address questions about spatiotemporal variability in CH_4 emissions.

2.1 SITES Water lakes

The SITES Water GHG Flux Program was established at five SITES Stations (lakes); Abisko Scientific Research Station (Almbergasjön), Svartberget Research Station (Stortjärn), Erken Laboratory (Erken), Skogaryd Research Catchment (Erssjön), and Asa Research Station (Feresjön). The stations with corresponding lakes are listed from north to south (Abisko lat. 68.33°N to Asa lat. 57.18°N) and are located along a ca 1300 km latitudinal gradient in Sweden (Fig. 1). The respective lakes vary considerably in local environmental conditions, such as trophic status, temperature, and water color (Table 1). Water chemistry data including soluble reactive phosphorus (SRP), total nitrogen (TN), dissolved organic carbon (DOC), and electrical conductivity (EC) and nearby meteorological data for the five lakes which is used in this study is openly available on the SITES Data Portal (https://data.fieldsites.se/portal/). Briefly, Almbergasjön (ALM) is a subalpine arctic lake that is clear enough to host significant benthic primary production (Ask et al. 2009). Stortjärn (STO), which is also part of the Krycklan Catchment Study (Laudon et al. 2021), is a small humic lake surrounded by north boreal coniferous forest and peatland (Denfeld et al. 2020). Erken (ERK) is a relatively large lake located in an agricultural and mixed forest landscape (Pettersson 1990). Erssjön (ERS) is a small lake surrounded by peatland, agricultural land and hemiboreal forest in the western part of Sweden with relatively high precipitation (Natchimuthu et al. 2016). Feresjön (FER) is a small lake surrounded by south boreal coniferous forest (Urrutia-Cordero et al. 2024).

Table 1. Characteristics of the five SITES lakes included in the study listed according to latitude from north to south.

Station	Lake Abb.	Coord. (N, E°)	Alt. (m)	Surface area (km^2)	Max / Mean depth (m)	Mixing Type	Trophic Status	DOC ($mg\ L^{-1}$)	SRP ($\mu g\ L^{-1}$)	EC ($\mu S\ cm^{-1}$)
Abisko	ALM	68.33, 19.15	380	0.06	6 / 3	Polymictic	Oligo	4.0	1.0	35
Svartberget	STO	64.26, 19.76	284	0.04	7 / 3	Dimictic	Meso	26.3	3.1	19
Erken	ERK	59.85, 18.57	13	24	21 / 9	Dimictic	Meso	10.9	11.1	289
Skogaryd	ERS	58.37, 12.16	73	0.06	5 / 2	Dimictic	Meso	25.0	2.8	56
Asa	FER	57.17, 14.81	195	0.52	13.5 / 4	Dimictic	Oligo	9.8	1.4	47

https://doi.org/10.5194/essd-2026-141
Preprint. Discussion started: 19 March 2026

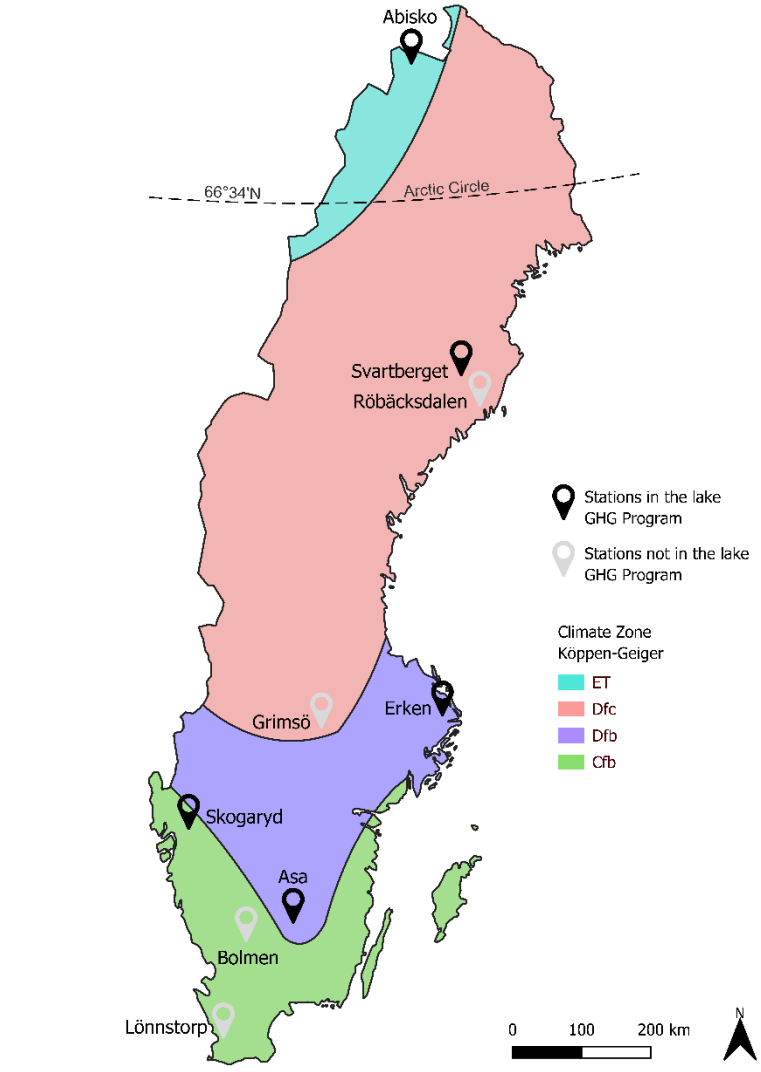

Figure 1. The locations and climate zones of all SITES research stations and in black the station harboring the studied lakes.

2.2 Lake CH_4 Flux Measurements

The CH_4 flux measurement design was based on findings that flux measurements for ~40 days, distributed over the year, with a minimum of 12 floating chambers, along depth transects, is needed to yield representative CH_4 flux data from open waters of small lakes (Natchimuthu et al. 2016, Peixoto et al. 2015, Wik et al., 2016). The SITES Water GHG Flux Program was run during the open water season with a bi-weekly sampling cycle for CH_4 flux. Due to the open water focus, measurements did not target CH_4 emissions connected to ice breakup. At the start of the sampling cycle, i.e. time 0, the chambers were set up on the lake. Floating chambers were placed on the water surface in three different transects starting from shore and extending towards the lake centre, thus covering different depth gradients per transect: 0-2 m, 2-4 m, and in some of the lakes > 4 m.

https://doi.org/10.5194/essd-2026-141
Preprint. Discussion started: 19 March 2026

There were 3-6 floating chambers per depth-zone and in total 12 chambers per lake and deployment period. At time 0 (start of chamber deployment), surface water samples for CH_4 were collected as well as air samples. Within 24-48 hours of deployment, headspace gas samples were collected from each chamber along with parallel surface water samples from the locations retrieved at the start of the monitoring as at time 0. Auxiliary data, including the time of chamber deployment (time 0) and sample collection (24-48 hours later) as well as water temperature, air temperature, and air pressure were collected on time 0 and upon chamber sampling and was used to calculate CH_4 concentration and flux.

Field sampling was conducted by staff at each of the five SITES stations. For surface water samples, 5 mL bubble-free surface water was collected with a syringe and added to a rubber-stopper capped 22 mL vial compatible with a vial headspace sampler for a gas chromatograph (see below). Prior to sampling, vials were prepared with acid (0.1 mL 85% analytical grade H_3PO_4) and filled with N_2, creating an overpressure in the vial, that was released prior to the water being added. Atmospheric air samples (3 x 60 mL) were collected 10 cm above the water surface with syringes. Around 160-170 mL of the total air sample was flushed through a capped storage vial, using the remaining ca. 10-20 mL to create overpressure of sample air that was added to the vial before the syringe was removed. Chamber gas samples were collected from the chambers by 60 mL syringes attached via a sampling tube and by gently pumping the first attached syringe to mix the gas content before extracting the gas sample. The 3 x 60 mL chamber headspace sample was added to the vial in the same manner as the air sample. Sample vials were stored dark and cool until analysis. The water and gas samples were analysed for CH_4 by gas chromatograph equipped with a Flame Ionization Detector (FID), and with auto-injection from vials by a headspace sampler. Overpressure in the vials was released prior to measurement on the GC. For detailed information on the sampling design and lab specifications see Swedish Infrastructure for Ecosystem Science (2026).

2.3 CH_4 flux calculations

Briefly, CH_4 concentrations in water or air were calculated from vial headspace partial pressures of CH_4 using Henry's law. The total CH_4 flux (F_{tot}) was calculated as the change in CH_4 concentrations between initial near-water-surface air samples and final chamber headspace samples using a non-linear model (see also Bastviken et al. 2004). Apparent k was estimated from the Fick´s flux equation

$$F = k \cdot (C_{aq} - C_{eq}), \quad \text{Eq. 1}$$

where F is CH_4 flux, C_{aq} is the surface water CH_4 concentration and C_{eq} is the theoretical surface water CH_4 concentration at equilibrium with the overlying air. To estimate diffusive CH_4 flux (F_{diff}), the chamber with the minimum apparent k was assumed to represent the minimum F_{diff}, provided that k was in a realistic range given the wind speed (see Bade 2009). Chambers with apparent k values up to 2-fold the minimum k were assumed to receive primarily F_{diff} as indicated previously

https://doi.org/10.5194/essd-2026-141
Preprint. Discussion started: 19 March 2026

(e.g. Bastviken et al. 2004, Schilder et al. 2013; 2016). The other chambers were assumed to receive both F_{diff} (estimated as the mean from the chambers dominated by F_{diff}) and ebullition (the remaining flux to reach F_{tot}) (Bastviken et al 2004). The F_{diff} and F_{tot} calculated by chambers were used to represent all flux data. The flux values in the data set are expressed in mmol m^{-2} d^{-1} and reflect the specific locations where the flux chambers were placed. Calculations of CH_4 surface water concentrations, fluxes, and apparent gas transfer velocities (k) are described in detail in supplemental calculation spreadsheet (Supplemental material). For data access see Swedish Infrastructure for Ecosystem Science (2026, https://doi.org/10.23700/05ax-st65).

Because of expected depth dependence for both ebullition and temperature effects (Natchimuthu et al. 2016), the mean flux (mmol m^{-2} d^{-1}) per depth-zone (n = 3-6 chambers per depth-zone and deployment period) was calculated. The temperature influence on total and diffusive fluxes was assessed for these different depth-zone fluxes separately using

$$F = F_{20} \cdot \theta^{(T-20)}, \quad \text{Eq. 2}$$

where F_{20} is the temperature normalized flux at 20 °C, and θ is the temperature response factor (Aben et al. 2017). The depth-zone specific fluxes were multiplied with the depth-zone area fraction and summed to determine whole-lake depth-zone weighted mean flux (accounting for differences among depth-zones and their respective area). Lake- and depth-zone specific versions of Eq. 2 were used to generate relationships between daily fluxes from the surface water temperature. Integrated whole lake fluxes (sometimes expressed per m^2 for comparability among lakes) were determined by summing the area-normalized fluxes from each depth-zone, accounting for both their different flux rates and their different area relative to the whole lake area. The depth-zone or whole-lake integrated fluxes reported represent depth-zone area mean flux or depth-zone area normalized whole lake mean flux, respectively, also expressed in mmol m^{-2} d^{-1}.

2.4 Data application example – using temperature to extrapolate fluxes over time

2.4.1. Surface water temperatures

To develop general relationships between water temperature and CH_4 emissions that could be used for gap filling and extrapolation, there is a need for long-term consistent daily surface water temperature data. Interpolated hourly air temperatures at 10 m above ground by coordinate (2.5 km grids) was downloaded from the Swedish Meteorological and Hydrological Institute (MESAN data; see https://www.smhi.se/data/om-smhis-data/uppdateringar-oppna-data/uppdateringar-i-smhis-oppna-data/2024-01-18-ny-version-av-api-for-meteorologiska-analyser-mesan) representing a seamless, consistent and verified air temperature data set for all lakes. To translate this spatiotemporally consistent air temperature data to surface water temperature, we developed lake-specific multiple regressions between the observed surface water CH_4 concentrations and three MESAN temperatures, the same hour, 24 hours earlier, and 120 hours earlier, according to

https://doi.org/10.5194/essd-2026-141
Preprint. Discussion started: 19 March 2026

Open Access Earth System Science Data Discussions

$$T_w = a * TAM\_120h + b * TAM\_24h + c * TAM + d, \quad \text{Eq. 3}$$

where T_w is surface water temperature, *TAM_120h* and *TAM_24h* are MESAN air temperatures 120 and 24 hours prior to the time of T_w and *TAM*. The parameters *a*, *b*, *c*, and *d*, were fitted using the observed T_w. This simple model yielded root mean square errors ranging from 1.2 to 1.6°C which is close to the uncertainty of approximately 1°C by more advanced hybrid models such as *air2water*, relying on lake heat budget calculations (Zhu et al. 2023). Hourly T_w was calculated for all days during the period of 2016-2022. To test for potential relationships with measured CH_4 fluxes, the T_w time series were resampled to match the chamber deployment time and thereafter averaged for the specific chamber deployment periods for which equivalent mean fluxes were generated.

2.4.2 Whole lake CH_4 flux estimation and uncertainty propagation

The uncertainty of the temperature relationships for F_{tot} are highly dependent on the fundamental uncertainty of ebullition which is strongly linked to the episodic nature of bubble release and the probability that bubbles are captured at the location and timing of the measurements. Accordingly, the uncertainty of the T_w-F_{tot} relationships reflect many more aspects than only T_w. Therefore, we used Monte Carlo simulations to extrapolate F_{tot} over time, while accounting for the various types of uncertainty projected onto F_{20} and θ in Eq. 2. Independent random extractions from the separate uncertainty distributions of F_{20} and θ was made 1000 times, thereby generating 1000 different versions of Eq. 2 for each lake to calculate F_{tot} for the years 2016-2022. Such calculations were made for the open water periods defined as the days of the year (DOYs) having T_w at or above the lowest registered T_w from the respective lake upon flux observations to avoid the winter period when no observational data can support the simulations. The specific fluxes related to ice out and lake overturn periods were not considered here as it was beyond the scope of this work. The whole lake depth-zone area normalized daily mean fluxes per m^2 were multiplied with the lake area and summed over all relevant DOYs for each year and these 1000 whole-lake yearly fluxes were used to estimate means and uncertainties.

2.5 Data processing and statistics

Data was processed in Python accessed via the Anaconda 3 package. Eq. 2 and Eq. 3 were parameterized from observed data using the scipy.optimize curve_fit tool. For comparing temperature-normalised fluxes (F_{20}) and θ among depth-zones across all lakes simultaneously, z-scores (a measure of how many standard deviations a data point is from the mean) of F_{20} and θ were calculated for each lake separately. Statistical comparisons among depth-zones and among years were performed using the analyse function in GraphPad Prism 10.0.2.

https://doi.org/10.5194/essd-2026-141
Preprint. Discussion started: 19 March 2026

Open Access Earth System Science Data Discussions

3 Results and discussion

3.1. General CH_4 Flux patterns

The SITES Water GHG Flux Program efforts in the five lakes between 2016-2022 resulted in 2375 unique CH_4 flux measurements (Table 2). The data distribution over time during years and over day-of-year (DOY) for combined years are shown in Fig. 2 and in Fig. A1. Overall, F_{tot}, F_{diff}, and C_{aq} ranges were 0.001 – 42.1 mmol m^{-2} d^{-1}, 0.001 – 1.77 mmol m^{-2} d^{-1}, and 0.01 – 4.3 µM, respectively. Such ranges are expected considering previous observations and align with the notion of great expected influence of weather variability on high-resolution CH_4 flux data (Johnson et al. 2022; Natchimuthu et al. 2014). F_{tot}, F_{diff}, and C_{aq} were all greatest in the most phosphorous-rich lake (ERK) and lowest in the arctic oligotrophic lake (ALM) which also featured the lowest temperatures (Table 1, Table 2). F_{diff} corresponded to 62% of the total flux in ALM. In the other lakes F_{diff} accounted for 19-36% of the F_{tot}. This means that ebullition only made up 38% in the most northern arctic lake ALM but dominated in all other lakes with contributions ranging from 64 to 81% of F_{tot} (Table 2).

Table 2. Overview of CH_4 flux measurements between 2016-2022 and mean surface water concentrations (C_{aq}) and CH_4 fluxes in the five SITES Water lakes studied. F_{diff} and F_{tot} are diffusive and total flux, respectively. "cmb" denote that values are from individual measurements at specific chambers and "dza" denotes that values were depth-zone-integrated and area-weighted. Values reported are based on observations only (i.e., no extrapolations).

	ALM	STO	ERK	ERS	FER
# of years	4	6	5	7	3
# of sampling campaigns	24	33	47	82	26
# of calculated total fluxes	230	440	542	887	276
C_{aq} (µM; cmb)					
Min – Max	0.01 – 0.31	0.06 – 2.93	0.09 – 4.3	0.05 – 3.20	0.04 – 1.58
Mean ± SD	0.10 ± 0.05	0.36 ± 0.22	0.80 ± 0.63	0.44 ± 0.31	0.20 ± 0.24
F_{diff} (mmol m^{-2} d^{-1}; cmb)					
Min – Max	0.001 – 0.091	0.01 – 0.30	0.02 – 1.77	0.005 – 0.72	0.01 – 0.80
Mean ± SD	0.015 ± 0.017	0.07 ± 0.06	0.25 ± 0.23	0.10 ± 0.09	0.16 ± 0.14
F_{tot} (mmol m^{-2} d^{-1}; cmb)					
Min – Max	0.001 – 0.137	0.01 – 9.5	0.02 – 42.1	0.01 – 12.1	0.01 – 28.9
Mean ± SD	0.024 ± 0.023	0.40 ± 0.97	1.85 ± 4.27	0.41 ± 0.95	1.06 ± 2.52
C_{aq} (µM; dza)					
Min – Max	0.03 – 0.18	0.18 – 0.69	0.18 – 2.01	0.08 – 0.71	0.07 – 1.38
Mean ± SD	0.10 ± 0.05	0.34 ± 0.12	0.85 ± 0.46	0.34 ± 0.15	0.21 ± 0.25
F_{diff} (mmol m^{-2} d^{-1}; dza)					
Min – Max	0.001 – 0.068	0.02 – 0.21	0.02 – 0.6	0.01 – 0.30	0.02 – 0.48
Mean ± SD	0.016 ± 0.017	0.08 ± 0.06	0.26 ± 0.16	0.09 ± 0.07	0.14 ± 0.12
F_{tot} (mmol m^{-2} d^{-1}; dza)					
Min – Max	0.007 – 0.073	0.06 – 1.23	0.09 – 6.72	0.02 – 0.70	0.05 – 1.97

https://doi.org/10.5194/essd-2026-141
Preprint. Discussion started: 19 March 2026

Mean ± SD	0.026 ± 0.018	0.37 ± 0.30	1.36 ± 1.41	0.25 ± 0.20	0.75 ± 0.58

Overall, F_{tot} and F_{diff} were highly variable (Fig. 2; Table 2), which is in line with findings from previous studies and can be explained by the large number of influencing physical, chemical and biological processes (Segers 1998; Rudd et al. 1974; Bastviken et al. 2022). The standard deviations were as large as the means, or even higher for total flux, which also includes ebullition known to be highly variable (Table 2). High variability in these data is to be expected in extensive and spatiotemporally representative data sets, especially when total lake CH_4 fluxes are largely driven by extreme flux events (e.g. ebullition). This dependency on extreme outliers for the total CH_4 mass transport from lakes to the atmosphere is mechanistically valid and important for accurate lake CH_4 emission assessments. Hence, representative accounting for such outlier fluxes becomes important is both measurement design and data processing.

https://doi.org/10.5194/essd-2026-141
Preprint. Discussion started: 19 March 2026

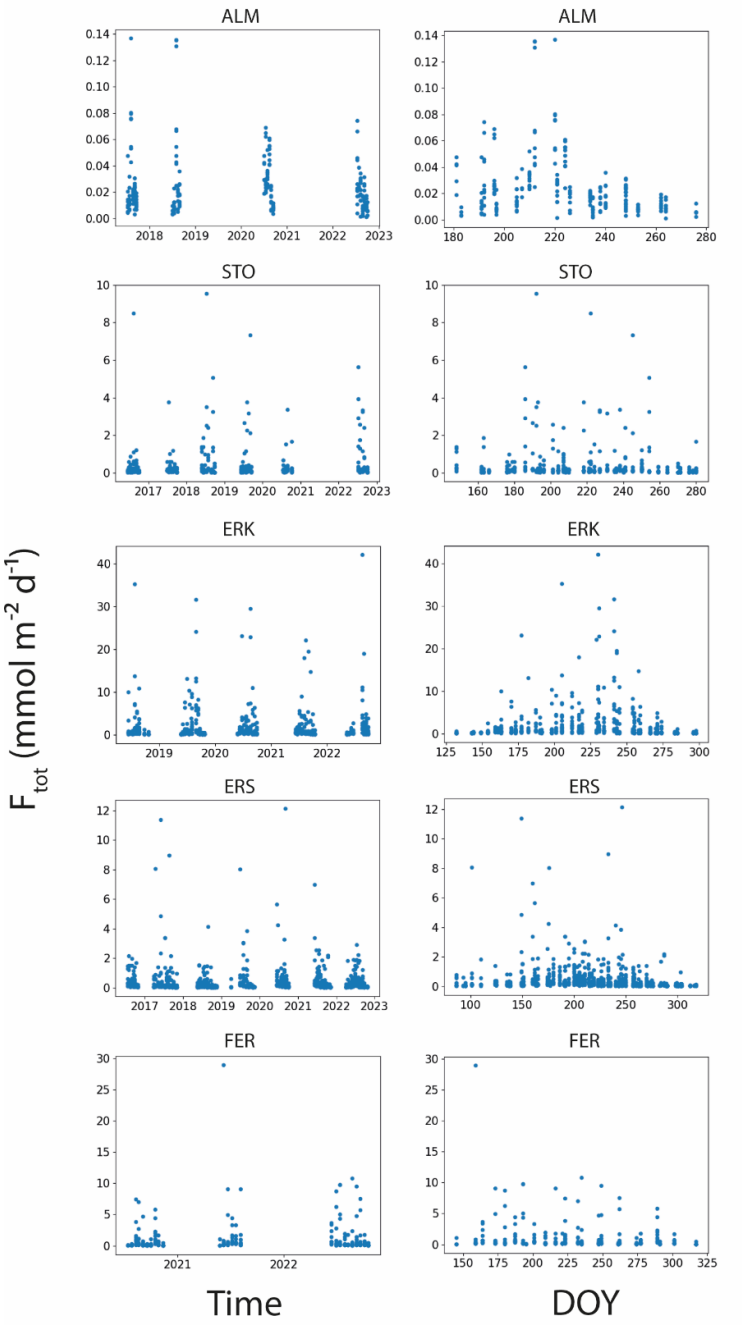

255 Figure 2. All measurements (n=2375) of total CH_4 flux (mmol m^{-2} d^{-1}) over time (left) and day-of-year (DOY, right) for all years. The time shown is the start time of the chamber deployments. Note the different scales on x- and y-axes. The lake name abbreviations are provided in Table 1 and the number of measurements in each lake is provided in Table 2.

https://doi.org/10.5194/essd-2026-141
Preprint. Discussion started: 19 March 2026

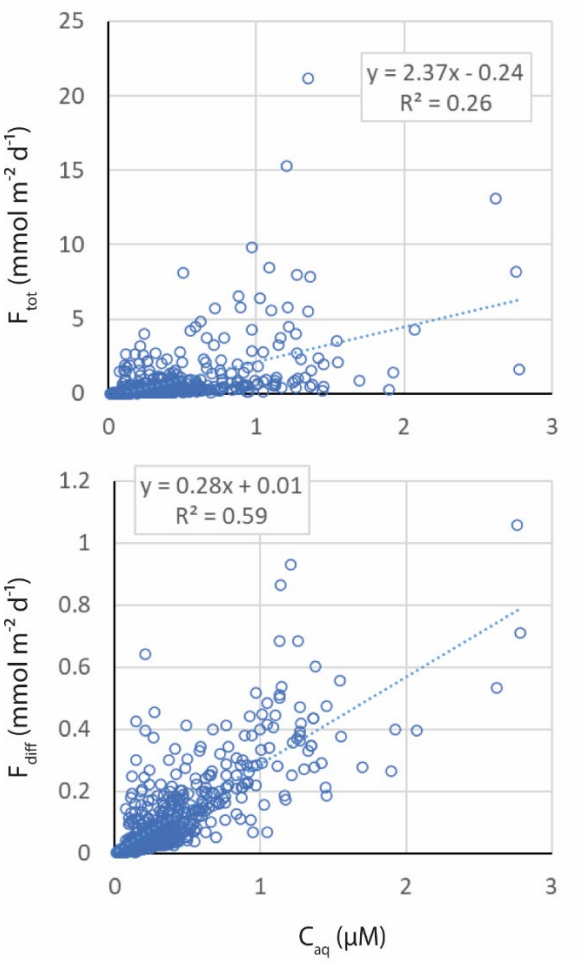

Figure 3. Depth-zone averaged total and diffusive CH_4 flux (F_{tot}, and F_{diff}) as a function of surface water CH_4 concentration (C_{aq}). Data presented include all five SITES lakes and measurements conducted at all dates. Regression equations and R^2 are shown in the respective panel.

While total individual instantaneous F_{tot} varied 100- to 1000-fold across space and time, F_{diff} varied 50- to 200-fold and C_{aq} varied 30- to 60-fold (Table 2). Accordingly, when considering depth-zone averaged values from all lakes and times, C_{aq} explained 26 and 59%, respectively of F_{tot} and F_{diff} (Fig. 3). This highlights that C_{aq} alone was not adequate to predict F_{tot}.

3.2. Within-lake spatiotemporal depth-zone patterns

The depth-zones constituted an important spatial feature. The highest F_{tot} came from depth-zone 0-2 m in all lakes, except for ERK, where they came from 2-4 m (Table A1). Because ERK is large in area and highly exposed to wind, it is possible that sediments in the shallowest zones were to a higher degree than in the other lakes re-suspended and transported to greater depths by wave action. If so, the shallowest sediments may be less rich in substrates favouring methanogenesis, which would agree

https://doi.org/10.5194/essd-2026-141
Preprint. Discussion started: 19 March 2026

with less release of bubbles from the shallowest depth-zone (Fig. 4; Table A2). In the smaller boreal or temperate lakes (STO, ERS, and FER), the pattern was clear with higher F_{tot} associated with the shallowest depth-zone, while the pattern was less pronounced in the subarctic lake (ALM), although still significant (Table A1). The notion that ebullition is depth-dependent has been suggested previously (e.g. Bastviken et al. 2004) but here we show this for F_{tot} based on more systematic multi-year data from multiple different lake types. Such depth-dependent patterns were also found for F_{diff} and C_{aq} in two of the lakes (ERS and FER; Table A1). The depth-zone influence on the measured fluxes implies that whole-lake CH_4 emission estimates need to be based on observations across different depths and that whole-lake CH_4 fluxes should be weighted to the relative areas of different depth-zones. Otherwise, the reported fluxes will likely be biased, as illustrated by comparing data in the upper and lower part of Table 2. The strongest bias in this data set was found for ERS where the mean F_{tot} of 0.41 mmol m^{-2} d^{-1} from all individual measurements should be compared with the 0.25 mmol m^{-2} d^{-1} (39% reduction) after depth-zone area-weighing. Accordingly, it is also important to report data in ways that make it clear if, and in such case also how within-lake depth distribution was considered, and how extrapolation to whole lake estimates was made.

Some of the temporal variability in F_{tot} was related to seasonality (Fig. 2) in agreement with previous long-term studies (Wik et al. 2016, Natichimuthu et al. 2016, Denfeld et al. 2020). Both the average F_{tot} and F_{diff} and the flux variability associated with ebullition were greater during the peak summer period than in other seasons (Fig. 2). In ERK, the seasonal patterns for C_{aq} were similar to the fluxes, but this pattern was less pronounced for the other lakes (Fig. A1). The seasonal patterns translate into apparent temperature relationships, which for F_{tot} were in most cases statistically significant, albeit weakened by the high flux variability (Fig. 4; Table A2). In ERK, ERS and FER, significant temperature relationships were found also for F_{diff}, and near-significant tendencies were observed also in the other lakes (Table A2). Similar exponential relationships have previously been observed in globally distributed ebullition studies (Bastviken and Johnson 2025; Aben et al. 2017; Wik et al. 2016; Yvon-Durocher et al. 2014), while consistent evidence for an apparent and general temperature relationship for F_{diff} based on *in situ* measurements are rarer (Aben et al. 2017; Johnson et al. 2022). Using the time series data from the five study lakes shows that *in situ*-based temperature–F_{diff} relationships can be observed based on direct flux measurements, at least in some lakes and for some depth-zones (Figure 4; Table A2).

The apparent temperature relationships integrate the response on CH_4 flux to several underlying factors including the intrinsic temperature sensitivity of chemical reaction rates including CH_4 production and oxidation, and physical effects such as solubility, as well as elevated substrate supply during summer (Yvon-Durocher et al. 2014; Marotta et al. 2014; Natchimuthu et al. 2016). This complexity is acknowledged for all aspects of temperature sensitivity in this study and can possibly be seen as a weakness as mechanistic insights will be limited. In contrast, it can also be seen as a strength that the temperature sensitivity results, based on direct flux measurements, integrates effects of all temperature-correlated factors and their potential interactions in the full *in situ* complexity.

https://doi.org/10.5194/essd-2026-141
Preprint. Discussion started: 19 March 2026

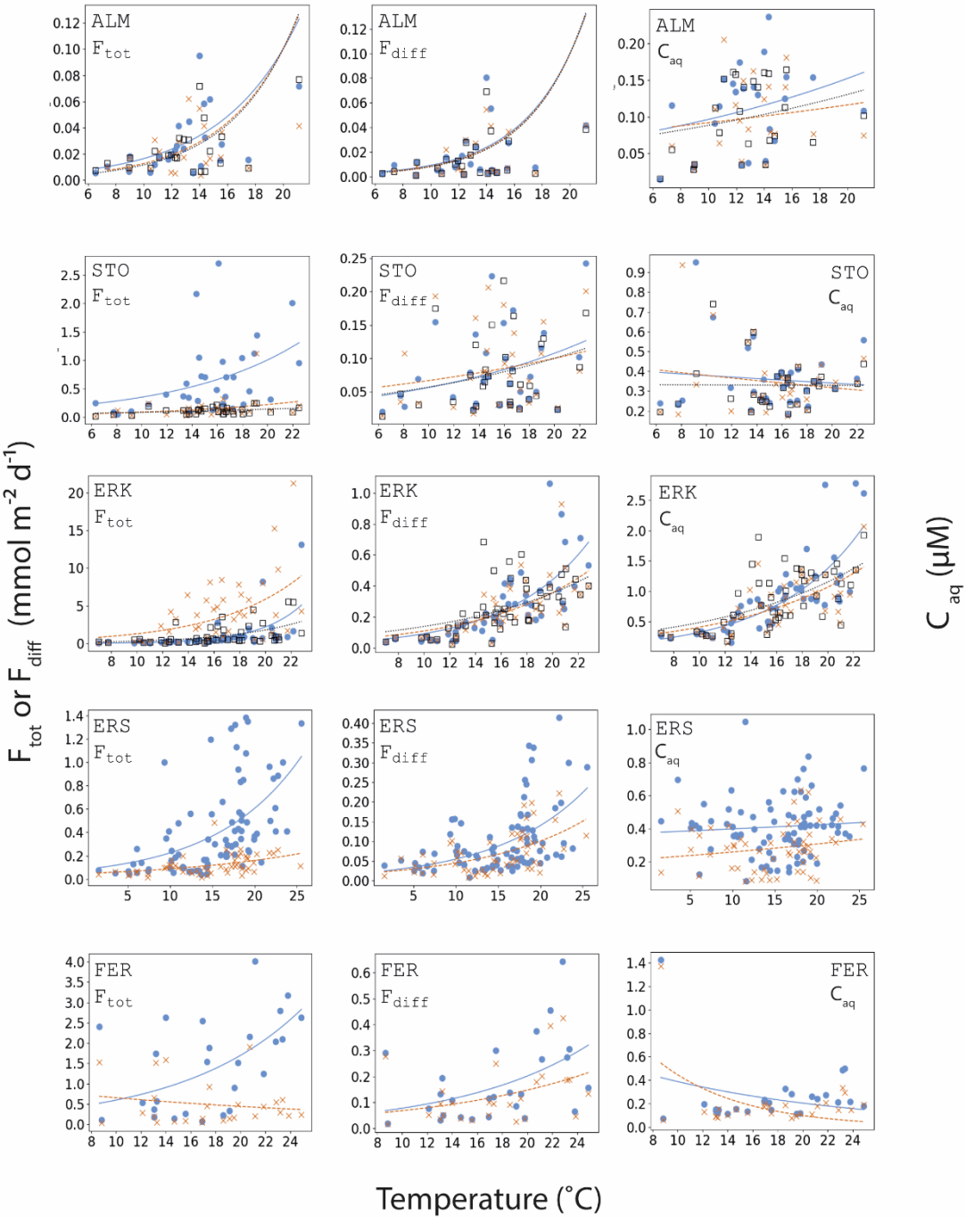

Figure 4. Mean total (left) and diffusive (center) CH_4 flux (mmol m^{-2} d^{-1}), and surface water CH_4 concentration (µM; right) by depth-zone and measurement occasion as function of water temperature (C) per lake. Blue points and solid lines denote a depth of 0-2 m, brown crosses and striped lines denote 2-4 m, and black open squares and dotted lines show > 4 m depth. n = 3-6 per depth-zone and measurement occasion.

https://doi.org/10.5194/essd-2026-141
Preprint. Discussion started: 19 March 2026

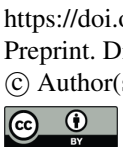

Open Access Earth System Science Data Discussions

Z-scores for F_{20}, representing the 20°C normalized flux, θ, and C_{aq} are shown in Fig. 5. Because the number of observations is small (one value per lake and depth-zone), statistically significant differences cannot be expected, but the tendency of greater values closer to the shore were apparent and particularly strong for F_{diff} and C_{aq}. The latter agrees with the highest CH_4 concentrations being observed at the shallowest depths (Table A1) and support past discoveries of a C_{aq} gradient with higher values near shore to lower values further offshore (e.g. Schilder et al. 2013). This could in turn explain greater near-shore F_{diff}, which provides support for a lateral transport of dissolved CH_4 from shores towards central parts of lakes.

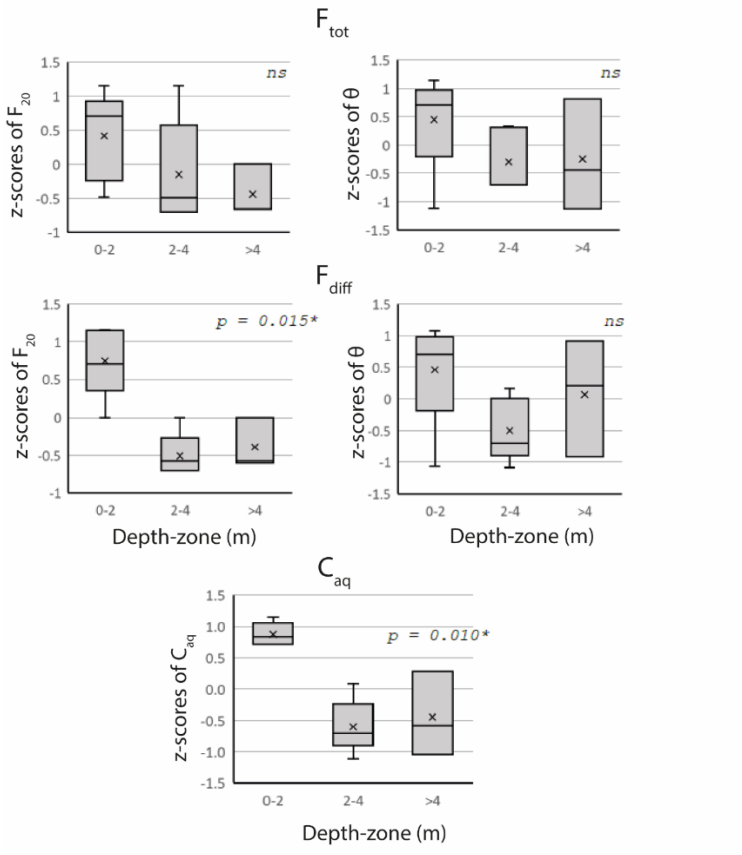

Figure 5. Z-scores of F_{20} (fluxes normalized to 20˚C) and θ (denoting temperature sensitivity) (left and right panels, respectively) by depth-zones for total and diffusive CH_4 flux (top and center, respectively) based on all flux measurements from the five SITES lakes. At the bottom the corresponding Z-scores of the surface water CH_4 concentrations (C_{aq}) are shown. The ”x” in the box plots show the mean values. There were statistically significant differences among depth-zones (denoted by ”ns”, α= 0.05) except for F_{20} for diffusive flux and for C_{aq} (one-way ANOVA with Greenhouse-Geisser correction).

The higher F_{20} and θ at shallow depths was particularly evident in small lakes surrounded by forest (STO, ERS, FER), suggesting an interaction between spatial (depth-zone) and temporal (temperature) features in at least some lakes (Table A2). This aligns with previous observations of higher and more temperature sensitive F_{tot} at the shallowest depths in ERS

https://doi.org/10.5194/essd-2026-141
Preprint. Discussion started: 19 March 2026

(Natchimuthu et al. 2016) but now also show that such a pattern is present also in other small lakes in the lake-rich northern temperate and boreal regions. Near-shore areas in small boreal lakes have also been found to receive substantial CH_4 inputs from the surrounding catchment in association with precipitation events (Denfeld et al. 2020).

3.3. Within-lake temporal patterns among years

Annual lake specific F_{tot} for the years 2016-2022 were derived for the open water period using the lake specific F_{tot}-temperature relationships to extrapolate between measurement occasions. The Monte Carlo based estimates showed large total uncertainty related to the high intrinsic variability of the F_{tot} observations. However, the Monte Carlo procedure to extract F_{20} and θ separately and independently from their respective distributions adds artefact uncertainty because F_{20} and θ are dependent parameter pairs. This overestimated uncertainty makes among-year comparisons conservative. Still, the simulated estimates showed statistically significant differences between specific years (one-way ANOVA with Tukeys' post-hoc comparison), with the exceptionally warm summer of 2018 (Wilcke et al. 2020) standing out as having the highest water temperatures and therefore also the highest F_{tot} (Fig. 6). Some of the yearly differences are generated from variable lengths of the open water periods (defined as water temperatures above the minimum water temperature of all flux measurement days on the respective lake), but most of the among-year variability seems associated with the mean water temperature for the corresponding period (Table A3). It is notable that an increase in mean water temperature of 0.5 to 3.2°C resulted in an estimated F_{tot} increase ranging from 16 to 74% with temperature sensitivities differing among lakes (Table A3). Such temperature responses are in line with previous *in situ* evidence of exponential temperature dependency on F_{tot} (Wik et al. 2016; Natchimuthu et al. 2016; Aben et al. 2017, Yvon-Durocher et al. 2014; Bastviken and Johnsson 2025). The result of this work contributes multi-year *in situ* temperature sensitivities from coordinated measurements across multiple lakes.

https://doi.org/10.5194/essd-2026-141
Preprint. Discussion started: 19 March 2026

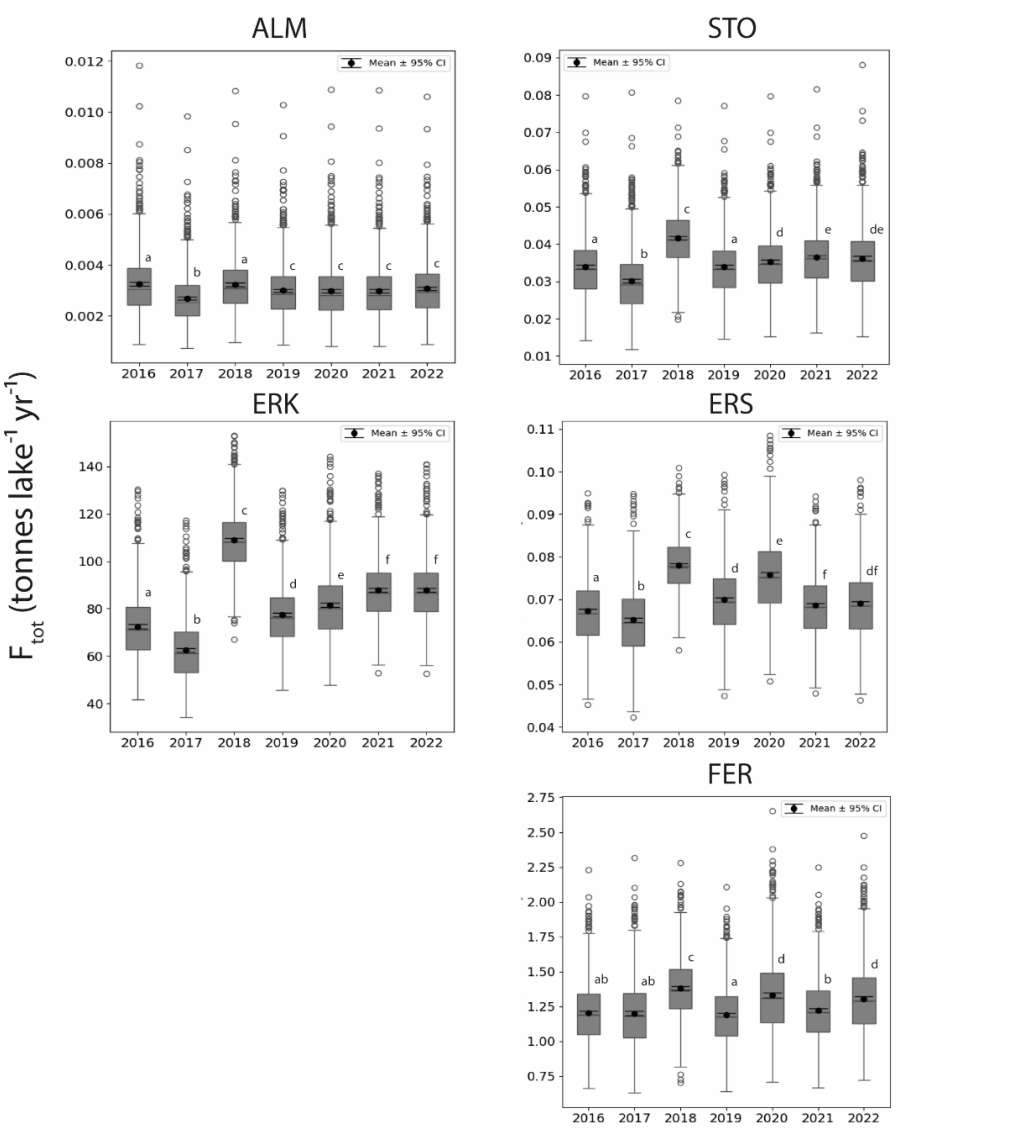

Figure 6. Simulated total CH_4 flux from the five SITES lakes from all days of years having a water temperature above the minimum temperature of the observational data. The simulation used the multi-year relationship between lake-specific water temperature as a function of depth-zone area normalized flux. The estimates and associated uncertainty were based on Monte Carlo simulations randomly extracting F_{20} and θ from their lake-specific distributions (N = 1000). Daily water temperature was modelled from the SMHI MESAN air temperature data as explained in the Methods. Note the different y-axis scales. Also note that the length of the integrated yearly number of days depends on how many days had a water temperature above the minimum threshold. This means that differences between years can be due to e.g. warm summer season periods (such as during 2018) or mild winters with more days above the temperature threshold. The letter combinations for each year denote statistically significant differences.

https://doi.org/10.5194/essd-2026-141
Preprint. Discussion started: 19 March 2026

3.4. Among-lake F_{tot} patterns

Comparisons among lakes rely on consistent extrapolation to whole lake fluxes. In this case the influence of the different depth-zones revealed the importance of accounting for depths zone differences and normalizing the depth-zone areas in consistent ways when generating whole lake integrated flux. For the open water period as defined here, the whole-lake F_{tot} (translated back to area-normalized daily fluxes for comparability among lakes) ranges were 0.003-0.072 (ALM), 0.11-1.38 (STO), 0.53-2.11 (ERK), 0.13-0.35 (ERS), and 0.32-1.42 (FER) mmol m^{-2} d^{-1}. The corresponding annual whole lake F_{tot} were 0.0027-0.0032 (ALM), 0.030-0.042 (STO), 62.5-108.8 (ERK), 0.065-0.078 (ERS), and 1.19-1.38 (FER) tonnes CH_4 $lake^{-1}$. The whole-lake F_{tot} varied over time in response to temperature and length of the open water period (Table A3).

The rigorous whole-lake integration, based on the extensive multi-year data (2375 observations), reduces the number of F_{20} or θ to 5 for whole lakes or 13 for depth-zones. This makes it challenging to assess patterns in temperature normalized F_{tot} (F_{20}) or θ. Possible relationships between F_{20} or θ (target variables) and SRP, TN, DOC, and EC were investigated (Fig. A2-A5). There were potential positive relationships between F_{20} and SRP and EC (Fig. A2 and A5), with very similar patterns possibly illustrating a correlation between SRP and EC. However, this pattern relies exclusively on the high fluxes from ERK, and this skewed data distribution prevents us from drawing clear conclusions. If there is a pattern, it was most clear for F_{diff}. Positive relationships between nutrient concentrations or biological productivity and CH_4 fluxes from lakes and reservoirs have been suggested previously (e.g. Davidson et al. 2018; Deemer and Holgerson 2021). Regarding θ, the highest possibility for a relationship was observed for DOC (negative relationship; clearest for F_{diff}; Fig. A4). Possibly, lakes with higher DOC levels have darker water and shallower stratification depth, which in turn reduces the water volume and sediment area experiencing fluctuating water temperatures during summer.

4 Conclusions and future work

The SITES Water GHG Flux Program represents a unique effort to quantify and study lake GHG emissions in systematic, comprehensive, and methodologically coordinated ways, encompassing variability across space and time within and among multiple lakes. The CH_4 flux data produced are made available with open access for further analyses via the SITES data portal (https://data.fieldsites.se/portal/), and what is presented in this study is just the first years (2016-2022) of a still ongoing program. Nevertheless, this first analysis revealed multiple within- and among-lake CH_4 flux patterns. Some of the highlighted findings were:

- Ebullition represented a major component of total CH_4 fluxes in most studied lakes. Thus, total fluxes are driven largely by episodic extreme fluxes per area and time unit. In turn, this means that representative flux measurements require high coverage in time and space and means are preferred (over medians) to represent total fluxes from lakes.
- Water concentrations of CH_4 explained almost 60% of the variability in diffusive flux (F_{diff}), while not being adequate as predictor of total flux (F_{tot}) for lakes with considerable ebullition.

https://doi.org/10.5194/essd-2026-141
Preprint. Discussion started: 19 March 2026

- Temperature-normalized CH_4 fluxes (e.g. F_{20}) are suggested to use for representative flux comparisons within and between lakes
- Identified CH_4 flux patterns, including temperature influences on fluxes, varied among depth-zones and lakes in consistent ways for the small forest lakes. The arctic subalpine lake and the large mesotrophic lake displayed slightly different patterns, suggesting important additional roles of morphometry and sediment characteristics in regulating CH_4 fluxes.
- Both F_{20} and the whole-system integrated temperature sensitivity coefficient θ may vary depending on lake characteristics.
- The consistent temperature response among years on whole lake CH_4 fluxes resulted in substantially elevated flux estimates for warmer years during the period of 2016-2022.

These findings and linkages to other, yet unexplored information available in the open access data presented here, are expected to be highly useful for improved fundamental understanding and modelling of lake CH_4 emissions. Overall, this study illustrates the value of consistent lake CH_4 flux measurements that take variability across space and time into account, both within and among lakes. This type of coordinated measurement program allows for more reliable flux comparisons among systems. Such multi-lake measurements conduced over long time scales are vital for comprehensive process understanding at field-scales, which in turn is essential for predicting future changes in lake CH_4 emissions. With lakes being one of the globally greatest atmospheric CH_4 sources, also being highly sensitive to climate change, the development of representative and comparable in-situ lake CH_4 flux data is key to drive, calibrate, and validate models to understand climate feedbacks. Establishing and maintaining research infrastructures with measurement programs such as the SITES Water GHG Flux Program in all relevant biomes are indispensable for such data collection.

5 Data availability

The data is openly available on the SITES Data Portal: https://data.fieldsites.se/portal/ as a data collection (https://doi.org/10.23700/05ax-st65), which contains five data files (one per lake) and a descriptive documentation file on field sampling, analysis and data access. Data collected within SITES are openly available and can be used by anyone as long as the data are cited and appropriately acknowledged, following the instructions in the SITES Data Policy: https://data.fieldsites.se/licence. Any publication using this data set should include a statement in the acknowledgement, e.g. "This [study/report/dataset/etc.] uses the SITES Water Layer 6, Greenhouse Gas Flux Program - Lake methane flux Data Collection, which has been made possible by the Swedish Infrastructure for Ecosystem Science (SITES) funded by the Swedish Research Council."

https://doi.org/10.5194/essd-2026-141
Preprint. Discussion started: 19 March 2026

Author contributions

The SITES Water program was initiated by HL with the GHG Flux Program method design by DB and LK, with key input from many others within the SITES community (see Acknowledgments). The staff at the SITES stations (Abisko Scientific Research Station (EL, NR), Asa Research Station (NAJ), Erken Laboratory (WCM, SL), Skogaryd Research Catchment (AL, PW) and Svartberget (JT, HL) locally organized and carried out the field sampling. SB, KB, MBW and LK centrally led SITES and overall coordinated the SITES Water program. Data processing was carried out by JS and DB. The documentation of sampling and analyses as well as data publishing were made by BAD and HV. The writing of the paper was led by DB, with support from MBW, BAD, and HV. All authors contributed to the final manuscript.

Competing interests

The contact authors have declared that none of the authors have any competing interests.

Acknowledgments

The Swedish Infrastructure for Ecosystem Science (SITES) GHG Flux Program was established with key input from Ingrid Sundgren, Sivakiruthika Balathandayuthabani (former last name Natchimuthu), Nguyen Thanh Duc, Patrick Crill. Lab staff at Gothenburg University (Aila Schachinger, Josefina Carlberg) and SLU (Jonas Lundholm) and Linköping University (Ingrid Sundgren) are acknowledged for conducting GC-analyses. Simone Moras provided support in making GIS maps. We further acknowledge the numerous numbers of students and seasonally employed personnel that contributed to the field sampling. This study uses the SITES Water Layer 6, Greenhouse Gas Flux Program Lake methane flux Data Collection (https://doi.org/10.23700/05ax-st65), which has been made possible by the Swedish Infrastructure for Ecosystem Science (SITES) funded by the Swedish Research Council.

Financial support

The Swedish Infrastructure for Ecosystem Science (SITES), including the SITES Water GHG Flux Program, is funded through the Swedish Research Council (by grant numbers 2017-00635 and 2021-00164). DB and Linköping University participants acknowledged were supported by the European Research Council (ERC) Horizon 2020 (grant 725546 METLAKE), the Swedish Research Council grants 2016-04829 and 2022-03841, and FORMAS grant 2018-01794.

References

Aben, R. C. H., Barros, N., van Donk, E., Frenken, T., Hilt, S., Kazanjian, G., Lamers, L. P. M., Peeters, E. T. H. M., Roelofs, J. G. M., de Senerpont Domis, L. N., Stephan, S., Velthuis, M., Van de Waal, D. B., Wik, M., Thornton, B. F., Wilkinson,

https://doi.org/10.5194/essd-2026-141
Preprint. Discussion started: 19 March 2026

J., DelSontro, T., Kosten, S., Cross continental increase in methane ebullition under climate change. Nature Communications, 8, (1), 1682, 2017.

Ask, J., Karlsson, J., Persson, L., Ask, P., Byström, P., Jansson, M., Whole-lake estimates of carbon flux through algae and bacteria in benthic and pelagic habitats of clear-water lakes. Ecology, 90: 1923-1932. doi:10.1890/07-1855.1, 2009.

Bade D., Gas Exchange at the Air–Water Interface. Pages 70-78 in Likens GE, ed. Encyclopedia of Inland Water. Oxford: Elsevier, 2009.

Bastviken, D., Johnson, M. S., Future methane emissions from lakes and reservoirs. Nature Water. doi:10.1038/s44221-025-00532-6, 2025.

Bastviken, D., Wilk, J., Duc, N. T., Gålfalk, M., Karlson, M., Neset, T. S., Opach, T., Enrich-Prast, A., Sundgren, I., Critical method needs in measuring greenhouse gas fluxes. Environmental Research Letters, 17(10), 104009, 2022.

Bastviken, D., Cole, J., Pace, M., Tranvik, L., Methane emissions from lakes: Dependence of lake characteristics, two regional assessments, and a global estimate, Global Biogeochem. Cycles, 18, GB4009, doi:10.1029/2004GB002238, 2004.

Davidson, T. A., Audet, J., Jeppesen, E., Landkildehus, F., Lauridsen, T. L., Søndergaard, M., Syväranta, J., Synergy between nutrients and warming enhances methane ebullition from experimental lakes. Nature Climate Change, 8, (2), 156-160, 2018.

Deemer, B. R., Holgerson, M. A. Drivers of methane flux differ between lakes and reservoirs, complicating global upscaling efforts. Journal of Geophysical Research: Biogeosciences, 126, e2019JG005600. doi:10.1029/2019JG005600, 2021.

DelSontro, T., del Giorgio, P.A., Prairie, Y.T. No Longer a Paradox: The Interaction Between Physical Transport and Biological Processes Explains the Spatial Distribution of Surface Water Methane Within and Across Lakes. Ecosystems 21, 1073–1087, doi:10.1007/s10021-017-0205-1, 2018.

DelSontro, T., Boutet, L., St-Pierre, A., del Giorgio, P.A., Prairie, Y.T., Methane ebullition and diffusion from northern ponds and lakes regulated by the interaction between temperature and system productivity. Limnol. Oceanogr., 61: S62-S77. doi:10.1002/lno.10335, 2016.

Denfeld, B. A., Lupon, A., Sponseller, R. A., Laudon, H., Karlsson, J., Heterogeneous CO2 and CH4 patterns across space and time in a small boreal lake. Inland Waters, 10(3), 348–359. doi:10.1080/20442041.2020.1787765, 2020

Grasset, C., Mendonça, R., Villamor Saucedo, G., Bastviken, D., Roland, F., Sobek, S., Large but variable methane production in anoxic freshwater sediment upon addition of allochthonous and autochthonous organic matter. Limnol. Oceanogr., 63: 1488-1501. doi:10.1002/lno.10786, 2018.

Johnson, M. S., Matthews, E., Du, J., Genovese, V., Bastviken, D., Methane emission from global lakes: New spatiotemporal data and observation-driven modeling of methane dynamics indicates lower emissions. Journal of Geophysical Research: Biogeosciences, 127, e2022JG006793. doi: 10.1029/2022JG006793, 2022.

Kirschke, S., Bousquet, P., Ciais, P., Saunois, M., Canadell, J. G., Dlugokencky, E. J., Bergamaschi, P., Bergmann, D., Blake, D. R., Bruhwiler, L., Cameron-Smith, P., Castaldi, S., Chevallier, F., Feng, L., Fraser, A., Heimann, M., Hodson, E. L., Houweling, S., Josse, B., Fraser, P. J., Krummel, P. B., Lamarque, J.-F., Langenfelds, R. L., Le Quéré, C., Naik, V.,

https://doi.org/10.5194/essd-2026-141
Preprint. Discussion started: 19 March 2026

O'Doherty, S., Palmer, P. I., Pison, I., Plummer, D., Poulter, B., Prinn, R. G., Rigby, M., Ringeval, B., Santini, M., Schmidt, M., Shindell, D. T., Simpson, I. J., Spahni, R., Steele, L. P., Strode, S. A., Sudo, K., Szopa, S., van der Werf, G. R., Voulgarakis, A., van Weele, M., Weiss, R. F., Williams, J. E., Zeng, G., Three decades of global methane sources and sinks. Nat. Geosci., 6, (10), 813-823, 2013.

Laudon, H., Hasselquist, E. M., Peichl, M., Lindgren, K., Sponseller, R., Lidman, F., et al., Northern landscapes in transition: Evidence, approach and ways forward using the Krycklan Catchment Study. Hydrol. Processes, 35(4), e14170, 2021.

MacIntyre, S., Amaral, J. H. F., Melack, J. M., Enhanced turbulence in the upper mixed layer under light winds and heating: Implications for gas fluxes. Journal of Geophysical Research: Oceans, 126, e2020JC017026. doi:10.1029/2020JC017026, 2021.

MacIntyre, S., Amaral, J. H. F., Barbosa, P. M., Cortés, A., Forsberg, B. R., Melack, J. M., Turbulence and gas transfer velocities in sheltered flooded forests of the Amazon Basin. Geophysical Research Letters, 46, 9628–9636. doi:10.1029/2019GL083948, 2019.

Marotta, H., Pinho, L., Gudasz, C., Bastviken, D., Tranvik, L. J., Enrich-Prast, A., Greenhouse gas production in low-latitude lake sediments responds strongly to warming. Nature Climate Change, 4, (6), 467-470, 2014.

Mattson, M., Likens, G. Air pressure and methane fluxes, Nature 347, 718–719, doi:10.1038/347718b0, 1990.

Natchimuthu, S., Sundgren, I., Gålfalk, M., Klemedtsson, L., Crill, P., Danielsson, Å. and Bastviken, D., Spatio-temporal variability of lake CH4 fluxes and its influence on annual whole lake emission estimates. Limnol. Oceanogr., 61: S13-S26. doi:10.1002/lno.10222, 2016.

Natchimuthu, S., Panneer Selvam, B., Bastviken, D. Influence of weather variables on methane and carbon dioxide flux from a shallow pond. Biogeochemistry 119, 403–413, doi:10.1007/s10533-014-9976-z, 2014.

Peixoto RB, Machado-Silva F, Marotta H, Enrich-Prast A, Bastviken D, Spatial versus Day-To-Day Within-Lake Variability in Tropical Floodplain Lake CH4 Emissions – Developing Optimized Approaches to Representative Flux Measurements. PLOS ONE 10(4): e0123319. doi:10.1371/journal.pone.0123319, 2015.

Pettersson, K. The spring development of phytoplankton in Lake Erken: species composition, biomass, primary production and nutrient conditions — a review. Hydrobiologia 191, 9–14, doi:10.1007/BF00026033, 1990.

Rasilo, T., Prairie, Y., del Giorgio, P., Large-scale patterns in summer diffusive CH4 fluxes across boreal lakes, and contribution to diffusive C emissions. Global Change Biology. 21. doi:10.1111/gcb.12741, 2014.

Rudd, J. W. M., Hamilton, R. D., Campbell, N. E. R., Measurement of microbial oxidation of methane in lake water, Limnology and Oceanography, 3, doi:10.4319/lo.1974.19.3.0519, 1974.

Saunois, M., Martinez, A., Poulter, B., Zhang, Z., Raymond, P. A., Regnier, P., Canadell, J. G., Jackson, R. B., Patra, P. K., Bousquet, P., Ciais, P., Dlugokencky, E. J., Lan, X., Allen, G. H., Bastviken, D., Beerling, D. J., Belikov, D. A., Blake, D. R., Castaldi, S., Crippa, M., Deemer, B. R., Dennison, F., Etiope, G., Gedney, N., Höglund-Isaksson, L., Holgerson, M. A., Hopcroft, P. O., Hugelius, G., Ito, A., Jain, A. K., Janardanan, R., Johnson, M. S., Kleinen, T., Krummel, P. B., Lauerwald, R., Li, T., Liu, X., McDonald, K. C., Melton, J. R., Mühle, J., Müller, J., Murguia-Flores, F., Niwa, Y., Noce,

https://doi.org/10.5194/essd-2026-141
Preprint. Discussion started: 19 March 2026

S., Pan, S., Parker, R. J., Peng, C., Ramonet, M., Riley, W. J., Rocher-Ros, G., Rosentreter, J. A., Sasakawa, M., Segers, A., Smith, S. J., Stanley, E. H., Thanwerdas, J., Tian, H., Tsuruta, A., Tubiello, F. N., Weber, T. S., van der Werf, G. R., Worthy, D. E. J., Xi, Y., Yoshida, Y., Zhang, W., Zheng, B., Zhu, Q., Zhu, Q., Zhuang, Q., Global Methane Budget 2000–2020. Earth Syst. Sci. Data, 17, (5), 1873-1958, 2025.

Schilder, J., Bastviken, D., van Hardenbroek, M., Heiri, O., Spatiotemporal patterns in methane flux and gas transfer velocity at low wind speeds: Implications for upscaling studies on small lakes, J. Geophys. Res. Biogeosci., 121, 1456–1467, doi:10.1002/2016JG003346, 2016.

Schilder, J., Bastviken, D., van Hardenbroek, M., Kankaala, P., Rinta, P., Stötter, T., Heiri, O., Spatial heterogeneity and lake morphology affect diffusive greenhouse gas emission estimates of lakes, Geophys. Res. Lett., 40, 5752–5756, doi:10.1002/2013GL057669, 2013.

Segers, R. Methane production and methane consumption: a review of processes underlying wetland methane fluxes. Biogeochemistry 41, 23–51, doi:10.1023/A:1005929032764, 1998.

Swedish Infrastructure for Ecosystem Science, SITES Water Layer 6, Greenhouse Gas Flux Program - Lake methane flux Data Collection [data set], https://doi.org/10.23700/05ax-st65, 2026

Sø, J.S., Martinsen, K.T., Kragh, T., Sand-Jensen, K., Ebullition dominates high methane emissions globally across all lake sizes. Biogeochemistry 168, 43, doi:10.1007/s10533-025-01233-8, 2025.

Urrutia-Cordero, P., Langvall, O., Weyhenmeyer, G. A., Hylander, S., Lundgren, M., Papadopoulou, S., Striebel, M., Lind, L., Langenheder, S. Cyanobacteria can benefit from freshwater salinization following the collapse of dominant phytoplankton competitors and zooplankton herbivores. Freshwater Biology, 69, 1748–1759. doi:10.1111/fwb.14323, 2024.

Wik, M., Varner, R. K., Anthony, K. W., MacIntyre, S., Bastviken, D., Climate-sensitive northern lakes and ponds are critical components of methane release. Nat. Geosci., 9, (2), 99-105, 2016.

Wilcke, R. A. I., Kjellström, E., Lin, C., Matei, D., Moberg, A., Tyrlis, E., The extremely warm summer of 2018 in Sweden – set in a historical context. Earth Syst. Dynam., 11, (4), 1107-1121, 2020.

Yvon-Durocher, G., Allen, A. P., Bastviken, D., Conrad, R., Gudasz, C., St-Pierre, A., Thanh-Duc, N., del Giorgio, P. A., Methane fluxes show consistent temperature dependence across microbial to ecosystem scales. Nature, 507, (7493), 488-491, 2014.

Zhu, S., M. Ptak, M. Sojka, A. P. Piotrowski, and W. Luo, A simple approach to estimate lake surface water temperatures in Polish lowland lakes, Journal of Hydrology: Regional Studies, 48, 101468, doi:10.1016/j.ejrh.2023.101468, 2023.

https://doi.org/10.5194/essd-2026-141
Preprint. Discussion started: 19 March 2026

Open Access Earth System Science Data Discussions

555 # Appendix A

Table A1. Pairwise comparisons of total and diffusive flux (F_{tot} and F_{diff}, respectively; mmol m^{-2} d^{-1}) and surface water CH_4 concentrations (C_{aq}; µM) among depth-zones 0-2 m (I), 2-4 m (II) and >4 m (III). Mean values for each depth-zone and measurement day were used. Repeated measures ANOVA with Geisser-Greenhouse correction with Tukey's post-hoc comparisons or paired t-test were used depending on if data covered three or two depth-zones. Statistical significance at alpha = 0.05 is shown with bold style.

Lake	**p-value**			**Interpretation**
	***F*$_{tot}$**	***F*$_{diff}$**	***C*$_{aq}$**	
ALM	**0.048** (I > II&III)	0.21	0.13	Slightly higher F_{tot} from shallower depths.
STO	**<0.0001** (I > II&III)	0.18	0.09	Small forest lake. Higher F_{tot} from shallower dz. CH_4 released from shallow sediments by ebullition or dissolved in water can explain this pattern.
ERK	**<0.0001** **(**II > I&III)	0.29	0.11	Large wind-exposed lake. 0-2 m sediments wave-flushed making lower littoral (2-4 m) receive redistributed sediments and potentially being a hot zone for ebullition.
ERS	**<0.0001** (I > II)	**<0.0001** (I > II)	**<0.0001** (I > II)	Small lake. Higher F_{tot}, F_{diff}, and C_{aq} from shallower dz. CH_4 released from shallow sediments by ebullition or dissolved in water can explain this pattern.
FER	**<0.0001** (I > II)	**0.001** (I > II)	**<0.0001** (I > II)	Small forest lake. Higher F_{tot}, F_{diff}, and C_{aq} from shallower dz. CH_4 released from shallow sediments by ebullition or dissolved in water can explain this pattern.

https://doi.org/10.5194/essd-2026-141
Preprint. Discussion started: 19 March 2026

Open Access Earth System Science Data Discussions

Table A2 Parameters in the apparent flux temperature sensitivity relationships (F_{20} and θ in Eq 1), as well as root mean square error (RMSE) and p-values for the respective relationships. Separate relationships were generated for different depth-zones of the different lakes.

Lake	Depth-zone	Area fraction	F_{tot}				F_{diff}			
			F_{tot20}	θ	RMSE	p-value	F_{diff20}	θ	RMSE	p-value
ALM	0-2	0.29	0.10	1.20	0.02	0.014	0.10	1.27	0.03	0.123
ALM	2-4	0.31	0.10	1.23	0.03	0.209	0.10	1.28	0.03	0.083
ALM	>4	0.40	0.10	1.24	0.02	0.003	0.10	1.29	0.03	0.105
STO	0-2	0.43	1.01	1.11	0.58	0.020	0.11	1.07	0.05	0.074
STO	2-4	0.31	0.22	1.10	0.18	0.103	0.10	1.04	0.06	0.302
STO	>4	0.25	0.14	1.05	0.06	0.051	0.10	1.06	0.05	0.201
ERK	0-2	0.10	2.18	1.35	1.75	<0.001	0.44	1.17	0.15	<0.001
ERK	2-4	0.10	5.86	1.16	3.55	<0.001	0.36	1.13	0.13	<0.001
ERK	>4	0.80	1.79	1.19	1.17	<0.001	0.35	1.10	0.14	<0.001
ERS	0-2	0.42	0.61	1.10	0.31	<0.001	0.14	1.10	0.07	<0.001
ERS	>2*	0.58	0.16	1.06	0.08	<0.001	0.10	1.08	0.04	<0.001
FER	0-2	0.26	1.70	1.12	0.93	0.004	0.20	1.10	0.13	0.016
FER	>2*	0.74	0.44	0.96	0.53	0.433	0.15	1.08	0.10	0.053

*Chamber measurements at 2-4 m depth but the lake has areas deeper than 4 m. Hence, the extrapolation to whole lake emissions may not properly account for emissions from the areas deeper than 4 m. In ERS, the area with a depth >4 m is minor (9%), while in FER this area is 41%.

https://doi.org/10.5194/essd-2026-141
Preprint. Discussion started: 19 March 2026

Open Access Earth System Science Data Discussions

Table A3. Output from Monte Carlo simulation of CH_4 emissions by lake and year. For lake abbreviations, see text. DAYS denotes the number of days that had a water temperature (*Tw*) above the minimum observed temperature across all years on a day of flux measurement for each lake. Mean *Tw* is the estimated water temperature for these DAYS. F_{tot} is total CH_4 flux. SD, CI_{low}, and CI_{up} denote standard deviation and lower and upper bond of the 95% confidence interval based on 1000 Monte Carlo simulations. Δmax *Tw* is the maximum mean Tw difference among the years for each lake. Δmax F_{tot} is the change in emission from the year with the lowest Tw to the year with the highest Tw expressed as percent.

Lake	Year	DAYS	Mean *Tw* (°C)	F_{tot} (mean)	F_{tot} (SD)	F_{tot} (CI_{low})	F_{tot} (CI_{up})	Δmax *Tw* (°C)	Δmax F_{tot} (%)
					(tonnes CH_4 $lake^{-1}$)				
ALM	2016	155	11.33	0.0032	0.0012	0.0032	0.0033		
	2017	129	11.34	0.0027	0.0010	0.0026	0.0027		
	2018	144	11.82	0.0032	0.0011	0.0032	0.0033	0.51	121
	2019	137	11.79	0.0030	0.0011	0.0029	0.0031		
	2020	143	11.42	0.0030	0.0011	0.0029	0.0030		
	2021	142	11.31	0.0030	0.0011	0.0029	0.0030		
	2022	141	11.75	0.0031	0.0011	0.0030	0.0031		
STO	2016	157	14.31	0.034	0.008	0.033	0.034		
	2017	154	13.17	0.030	0.009	0.030	0.031		
	2018	160	15.73	0.042	0.008	0.041	0.042	2.56	138
	2019	152	14.42	0.034	0.008	0.033	0.034		
	2020	157	14.40	0.035	0.008	0.035	0.036		
	2021	160	14.31	0.037	0.008	0.036	0.037		
	2022	170	13.66	0.036	0.009	0.036	0.037		
ERK	2016	198	14.07	72.5	14.5	71.6	73.4		
	2017	179	14.12	62.5	13.7	61.6	63.3		
	2018	208	15.39	108.8	13.0	108.0	109.6	1.84	174
	2019	194	14.30	77.4	13.4	76.6	78.2		
	2020	224	13.55	81.6	15.1	80.6	82.5		
	2021	199	14.56	87.8	13.0	87.0	88.6		
	2022	210	14.26	88.0	13.5	87.1	88.8		
ERS	2016	304	11.75	0.067	0.008	0.067	0.068		
	2017	318	10.96	0.065	0.008	0.065	0.066		
	2018	266	14.16	0.078	0.006	0.078	0.078	3.20	120
	2019	328	11.07	0.070	0.008	0.069	0.070		
	2020	361	11.07	0.076	0.009	0.075	0.076		
	2021	293	12.16	0.069	0.007	0.068	0.069		
	2022	320	11.36	0.069	0.008	0.068	0.070		
FER	2016	196	16.31	1.20	0.23	1.19	1.22		
	2017	199	15.81	1.20	0.25	1.18	1.22		
	2018	216	17.61	1.38	0.23	1.36	1.39	2.08	116
	2019	192	16.74	1.19	0.22	1.18	1.20		
	2020	221	15.53	1.33	0.28	1.31	1.35		
	2021	198	16.44	1.22	0.23	1.21	1.24		
	2022	214	16.02	1.30	0.26	1.29	1.32		

https://doi.org/10.5194/essd-2026-141
Preprint. Discussion started: 19 March 2026

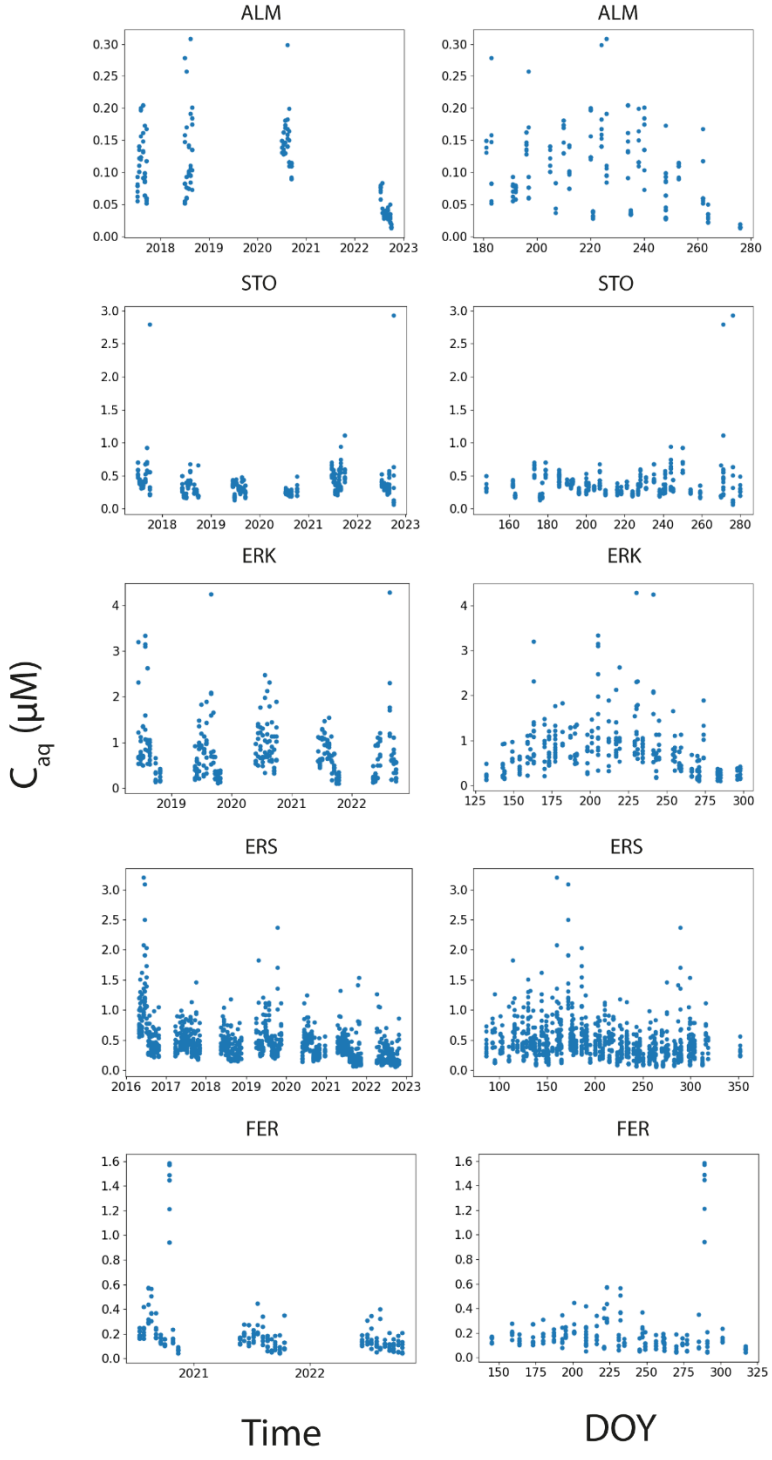

570 Figure A1. All measurements of surface water CH_4 concentrations (µM) over time and day-of-year (DOY) for all years (left and right panels. respectively). The time shown is the start time of the chamber deployments. The number of measurements in each lake is provided in Table 2.

https://doi.org/10.5194/essd-2026-141
Preprint. Discussion started: 19 March 2026

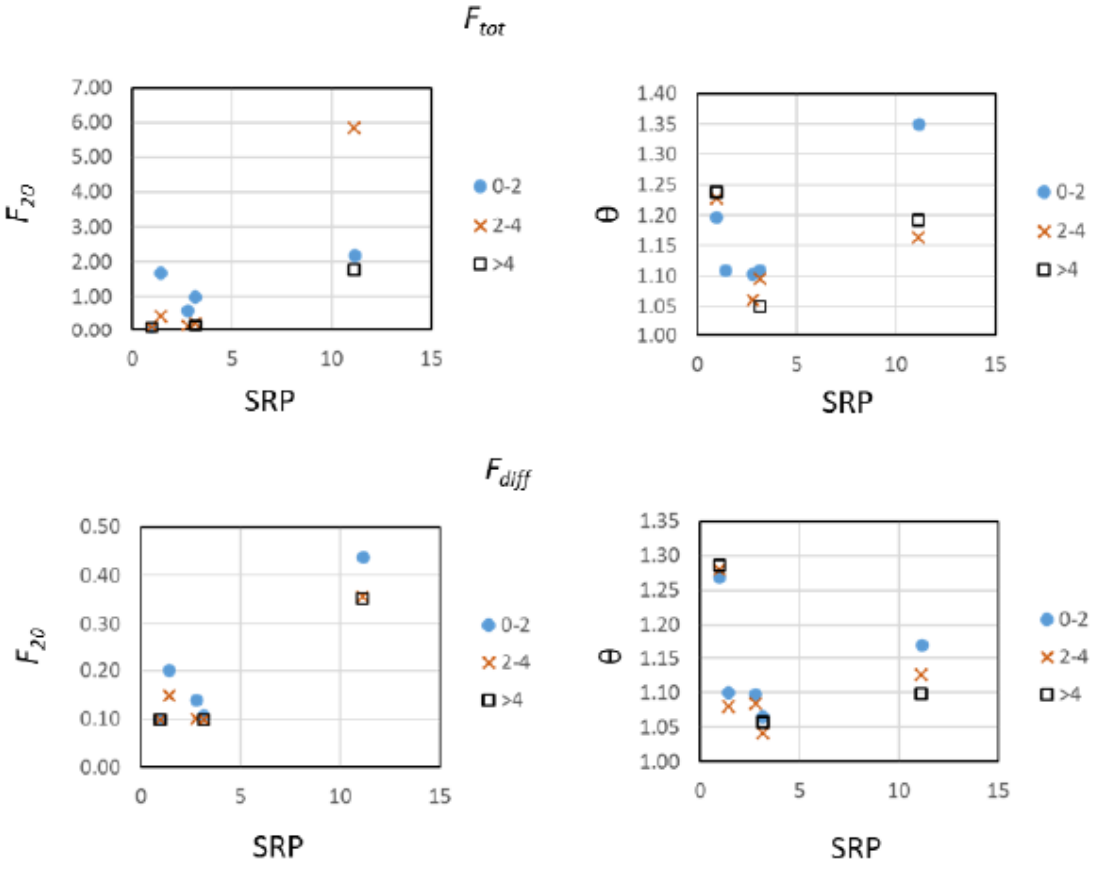

Figure A2. Temperature normalized CH_4 emissions (F_{20}) and the temperature sensitivity factor (θ) plotted as a function of mean surface water soluble reactive phosphorous (SRP; µg L^{-1}). Left panels show mean temperature normalized CH_4 emission (at 20˚C; F_{20}; mmol m^{-2} d^{-1}). Right panels show the θ temperature response factor (see Eq. 2). Top panels show fluxes and θ for the total emissions. bottom panels regard diffusive emissions. Blue points denote depths of 0-2 m. blown crosses denote 2-4 m. and black open squares show > 4 m depth.

https://doi.org/10.5194/essd-2026-141
Preprint. Discussion started: 19 March 2026

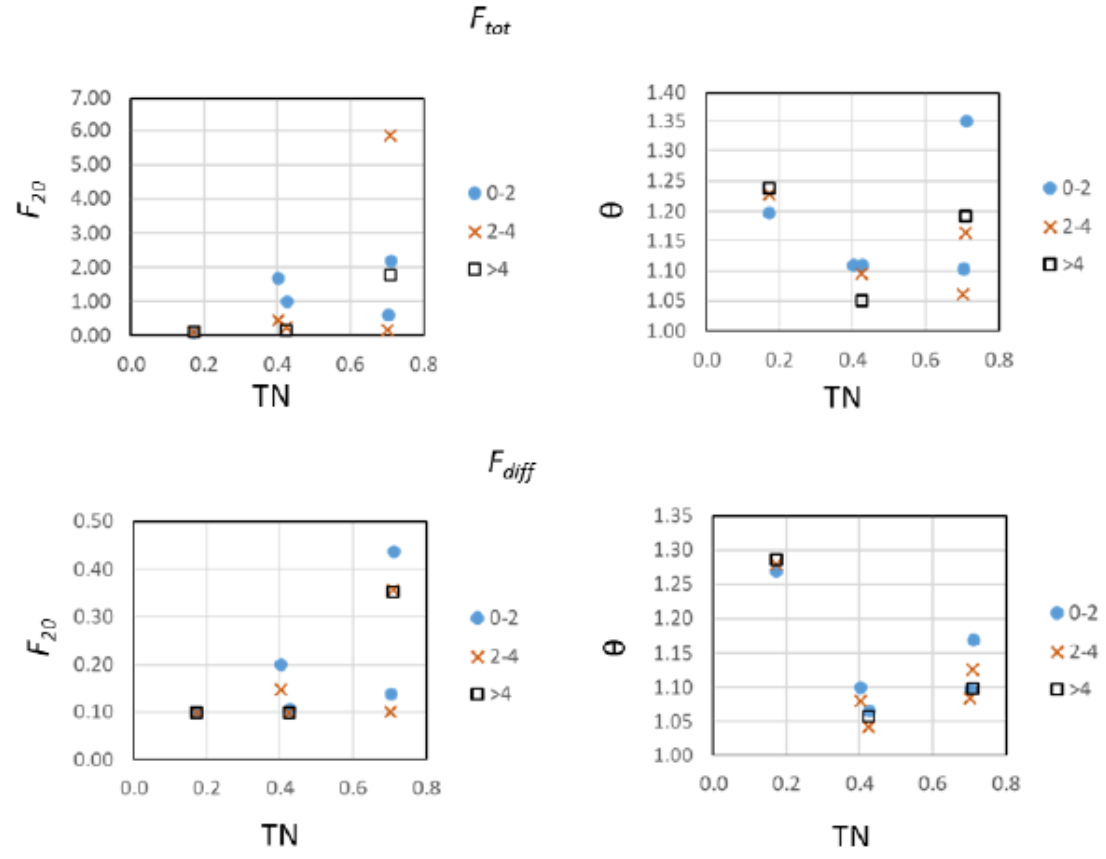

Figure A3. Temperature normalized CH_4 emissions (F_{20}) and the temperature sensitivity factor (θ) plotted as a function of mean surface water total nitrogen concentration (TN; mg L^{-1}). Left panels show mean temperature normalized CH_4 emission (at 20˚C; F_{20}; mmol m^{-2} d^{-1}). Right panels show the θ temperature response factor (see Eq. 2). Top panels show fluxes and θ for the total emissions. bottom panels regard diffusive emissions. Blue points denote depths of 0-2 m. blown crosses denote 2-4 m. and black open squares show > 4 m depth.

https://doi.org/10.5194/essd-2026-141
Preprint. Discussion started: 19 March 2026

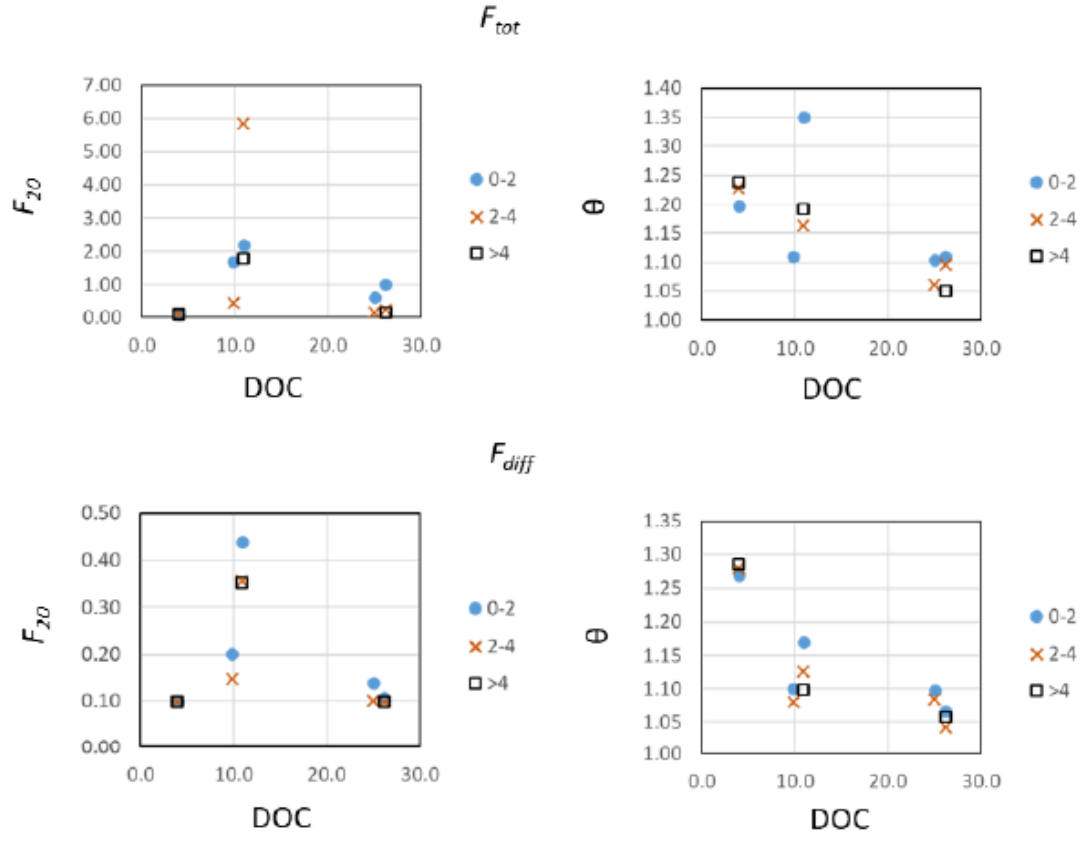

Figure A4. Temperature normalized CH_4 emissions (F_{20}) and the temperature sensitivity factor (θ) plotted as a function of mean surface water dissolved organic carbon (DOC; mg L^{-1}). Left panels show mean temperature normalized CH_4 emission (at 20˚C; F_{20}; mmol m^{-2} d^{-1}). Right panels show the θ temperature response factor (see Eq. 2). Top panels show fluxes and θ for the total emissions. bottom panels regard diffusive emissions. Blue points denote depths of 0-2 m. blown crosses denote 2-4 m. and black open squares show > 4 m depth.

https://doi.org/10.5194/essd-2026-141
Preprint. Discussion started: 19 March 2026

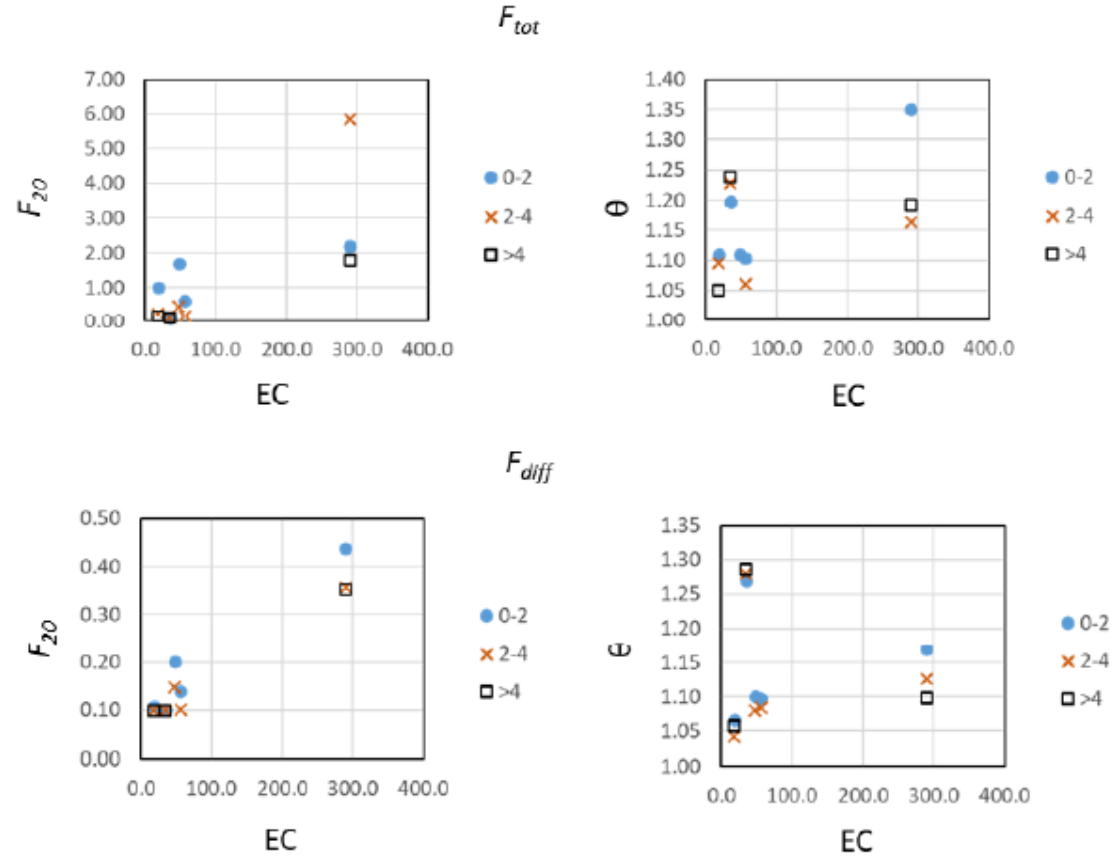

Figure A5. Temperature normalized CH_4 emissions (F_{20}) and the temperature sensitivity factor (θ) plotted as a function of mean surface water electrical conductivity (EC; µS cm^{-1}). Left panels show mean temperature normalized CH_4 emission (at 20˚C; F_{20}; mmol m^{-2} d^{-1}). Right panels show the θ temperature response factor (see Eq. 2). Top panels show fluxes and θ for the total emissions. bottom panels regard diffusive emissions. Blue points denote depths of 0-2 m. blown crosses denote 2-4 m. and black open squares show > 4 m depth.